ISSN 0018-151X, High Temperature, 2017, Vol. 55, No. 3, pp. 326–333. © Pleiades Publishing, Ltd., 2017.
Original Russian Text © N. Bonifaci, V.M. Atrazhev, V.A. Shakhatov, R.E. Boltnev, K. von Haeften, J. Eloranta, 2017, published in Teplofizika Vysokikh Temperatur, 2017, Vol. 55, No. 3, pp. 337–344.

PLASMA INVESTIGATIONS

Nonmonotonic Distribution of Population of the $a^3\Sigma_u^+$ Triplet State Rotational Levels in Corona Discharge in Cryogenic Helium Gas

N. Bonifaci[a], V. M. Atrazhev[b, *], V. A. Shakhatov[c], R. E. Boltnev[b, d], K. von Haeften[e], and J. Eloranta[f]

[a] *Laboratoire G2Elab CNRS & Grenoble University, Grenoble, France*
[b] *Joint Institute for High Temperatures, Russian Academy of Sciences, Moscow, 127412 Russia*
[c] *Topchiev Institute of Petrochemical Synthesis, Russian Academy of Sciences, Moscow, 119991 Russia*
[d] *Institute of Problems of Chemical Physics, Russian Academy of Sciences, Chernogolovka, Moscow region, 142432 Russia*
[e] *Department of Physics and Astronomy, University of Leicester, Leicester, UK*
[f] *Department of Chemistry and Biochemistry, University of Northridge, Northridge, USA*
**e-mail: atrazhev@yandex.ru*

Received October 8, 2015

Abstract—We observed the spectra within the wavelength range of 910–990 nm of emission of the corona discharge in supercritical helium gas at 6–11 K. This spectral range contains the molecular bands of the He_2^* excimer radiative transitions ($c^3\Sigma_g^+ \Rightarrow a^3\Sigma_u^+$) between the electron-vibrational-rotational levels of the $c^3\Sigma_g^+$ and the $a^3\Sigma_u^+$ triplet states. We have determined the populations of the rotational levels (quantity of molecules in the given excited state among the excited molecules of the discharge) of the $c^3\Sigma_g^+$ excited state from experimental values of the intensity of the respective electron-vibrational-rotational lines. The calculated population distribution is nonmonotonous. The population of the level with the rotation quantum number $K' = 18$ (the level number) is higher than those of the levels with the other K' values.

DOI: 10.1134/S0018151X1703004X

INTRODUCTION

We have analyzed the molecular spectral lines emitted at excitation of supercritical helium gas at 6 K. The helium luminescence was produced by means of the corona discharge near the electrode with the tip diameter of 2 μm under several kilovolts. The emission spectrum within the wavelength range of 910–990 nm was analyzed. This range contains the spectral electron-vibrational-rotational (EVR) lines of molecular bands of 0 sequence in the $c^3\Sigma_g^+ \Rightarrow a^3\Sigma_u^+$ system of the He_2^* excimer. The line intensities are proportional to the populations of the rotation levels of the upper $c^3\Sigma_g^+$ state. Thus, the first step of the observed spectra analysis consists in ascertainment of the correspondence between the spectral line wavelength of the level parameters (the rotational quantum number and the affiliation with the *P*- or the *R*-branch of the spectrum) and their numeration.

Earlier we studied the spectra in similar experiments performed in liquid helium at 4.2 K [1]. We observed several EVR-lines for the transitions from the lowest rotational levels of the singlet, $C^1\Sigma_g^+$, and the triplet, $c^3\Sigma_g^+$, states of the He_2^* excimer. Analysis of intensities of those lines makes it possible to calculate the populations of the rotational levels. The obtained population distribution decreases monotonously with the level number increase whereas the population distribution of the rotational levels of the equilibrium plasmas is described by the Boltzmann law with the rotational temperature close to the thermodynamic temperature of the medium. The corona discharge plasma is nonequilibrium and the population distribution of the rotational levels does not correspond to the Boltzmann distribution.

Cryogenic gas at 6 K has incomparably lower density resulting in low broadening of the spectral lines. In the present experiments, we observed the EVR-lines with the numbers above 20. Note that the lines with the numbers close to 18 are the most intensive. The lines with those numbers belonging to different spectral branches differ essentially in wavelengths, are located in different spectral ranges, and stand out against the background with their high intensity. We have discovered that high intensity of a number of the spectral lines is a consequence of the nonmonotonous population distribution of the levels, with the maximum for the 18-th level.

EXPERIMENT

The experimental facility is described in [2]; here, we present a short review of its peculiarities. The 99.9999% pure helium was additionally purified by means of transit through a number of cold traps with active carbon. Then, we filled up the high-pressure cell (standing the pressure up to 100 atm) with the purified helium. The cell was equipped with two windows and installed in the liquid helium cryostat at 4.2 K and above. We measured the temperature by means of the LakeShore GR-200A-2500 germanium thermometer (with accuracy of ±0.5 mK at 4.2 K) located on the flat copper electrode. Two high-voltage electrodes were embedded into the cell: the first one was the pointed tungsten tip, and, the second one, the flat plate at a distance of 8 mm from the tip end. The tungsten tips were prepared by electrolytic etching and had tip radii from 0.45 μm to 2.5 μm.

The electrodes were anchored on Marcor insulators. High DC voltage stabilized by the Spellman RHSR/20PN60 supply was applied to the tip electrode. The stationary corona discharge (similar to the corona discharge in the low-density gas) occurred near the tip. The lens on the input slit of the SpectraPro-300i spectrograph (focal length, 300 mm; aperture, f/4.0) were focused on the light emitted from the small area near the tip. The spectrograph was equipped with the three gratings (150 grooves/mm and two of 1200 gr./mm) to detect the spectra within the wavelength range near 750 nm and 300 nm, respectively. The 2D-CCDTKB-UV/AR sensor (12.3 × 12.3 mm, 512 × 512 pixels, 24 × 24 μm per each pixel) was installed directly at the spectrograph output. In order to reduce the parasitic current, we cooled the sensor to 153 K (the parasitic current was less than 1e/pixel per hour at 153 K). The slit broadening of the spectral lines measured from the profiles of the argon lines (obtained from the low-pressure discharge lamp) was $\Delta\lambda = 0.1$ nm for the 1200 gr./mm grating.

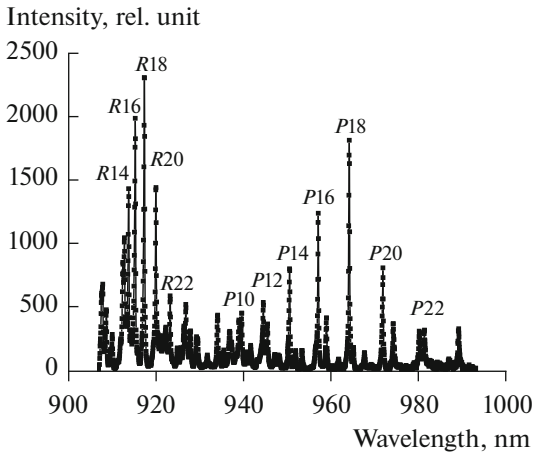

Fig. 1. Experimental spectrum within the wavelength range of 910–990 nm observed in the corona discharge in the supercritical helium gas at the temperature of 6 K and the pressure of 0.1 MPa.

EXPERIMENTAL RESULTS AND ANALYSIS

We performed the investigations within a wide range of thermodynamic states of helium from liquid at 4.2 K to gas at room temperature. We varied the gas medium density via variations of applied pressure, P. In the different experiments, we observed the spectra within the wide wavelength range of 500–1080 nm. In those spectra, we have identified the atomic lines and the molecular bands. The lines correspond to the radiative transitions between the excited states of the He* atoms or the He_2^* excimer molecules. At low pressure, the detected spectra contain the lines corresponding to the atomic lines and the molecular bands in the helium spectra obtained in experiments with rarefied gas. Above $P = 5.0$ MPa, strong background emission occurs. The line widths increase with the pressure increase and their relative intensity decreases. If the pressure exceeds 6.0 MPa, neither atomic lines nor molecular bands are observed in the spectra.

We observed the atomic lines and the molecular bands of helium in different experiments in liquid and in gaseous supercritical helium at temperatures above the critical temperature of 5.2 K. By means of the 1200 gr./mm grating, we obtained in liquid helium the high-resolution spectra clearly demonstrating the electron-vibrational-rotational structure of the molecular bands. This structure is resolved at pressures of 0.1–0.2 MPa. The nonresolved EVR-structure of the band registered at 0.6 MPa is reminiscent of the spectrum observed in [3] where the superfluid helium was irradiated by high-energy electrons. The spectral shift of the observed EVR-lines is in good agreement with experimental data [4] obtained for the superfluid HeII at 1.7 K. The EVR-structure of the bands of the $C^1\Sigma_g^+ \Rightarrow A^1\Sigma_u^+$ and the $c^3\Sigma_g^+ \Rightarrow a^3\Sigma_u^+$ systems resolved at pressures below 0.2 MPA is similar to the structure observed in the luminescence spectrum of the synchrotron irradiated liquid droplets [5].

In the present work, we discuss the spectrum obtained in the supercritical cryogenic helium gas at 6 K and pressure of 1 atm (Fig. 1). Here, the experimental wavelengths (the dots) are compared to their values in vacuum (the vertical bars). The line number is marked. We might clearly evolve two high-intensive EVR-line groups. The present work is aimed at explanation of that phenomenon. The line identification is the first step in the spectrum analysis.

STRUCTURE OF THE ROTATIONAL LEVELS OF THE MOLECULAR BANDS OF $c^3\Sigma_g^+ \Rightarrow a^3\Sigma_u^+$ SYSTEM

The symmetry properties and the electron-vibrational-rotational structure of the triplet and the singlet

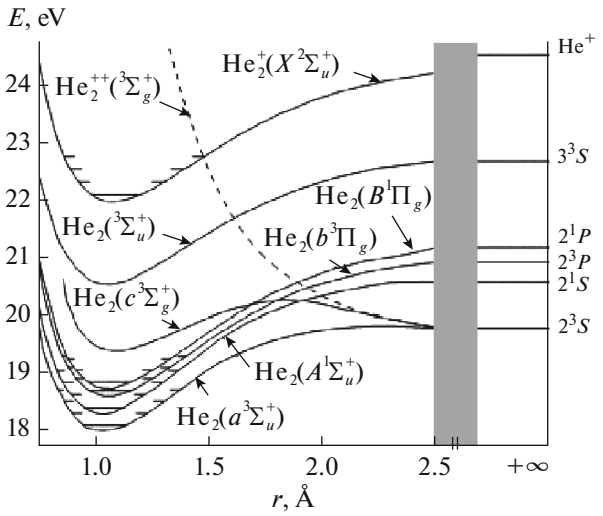

Fig. 2. Lower excited terms of the excimer, He_2^* produced via association of excited He* atom in the metastable 2^1S or 2^3S state with He atom in the ground state; at the right—the He atom levels [10].

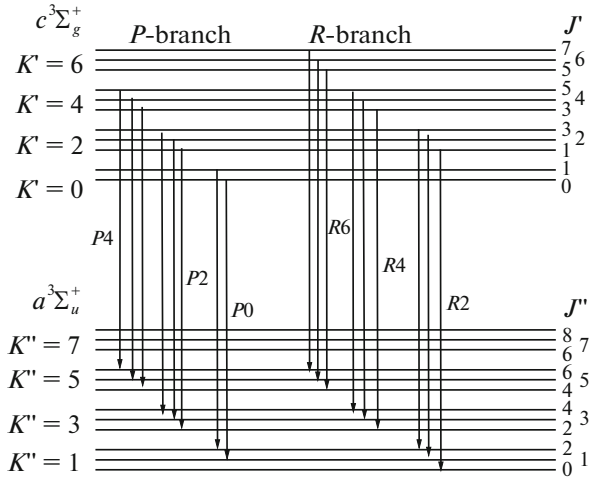

Fig. 3. Layout of rotational levels of the $c^3\Sigma_g^+$ and the $a^3\Sigma_u^+$ triplet terms and transitions between them: the *P*- and the *R*-branches; the quantum numbers of the upper levels, *K*', are the transition numbers.

states of the helium molecule was discussed in detail in [1]. Here, for clarity's sake, we present brief results of the EVR structure studies of emitting levels of the molecular bands of $c^3\Sigma_g^+ \Rightarrow a^3\Sigma_u^+$ system.

It is known in [6] that the electron-vibrational-rotational lines belonging to the sequence 0 of the singlet, $C^1\Sigma_g^+ \Rightarrow A^1\Sigma_u^+$, and the triplet, $c^3\Sigma_g^+ \Rightarrow a^3\Sigma_u^+$, systems of the He_2^* excimer molecule occupy the wavelength range of 910–990 nm. The $A^1\Sigma_u^+$ and $a^3\Sigma_u^+$ states are the lowest ones from the excited states of the He_2^* molecule; they are marked by arrows in Fig. 2.

The state of the molecule (the rotational level) is characterized by the rotational quantum number, $K = \Lambda + N$, where Λ is the projection of the electron orbital momentum on the internuclear axis of the molecule, and, *N*, the nuclear momentum; *K* is the total momentum of the molecule without account for the spin. The wave function of the He_2^* molecule (the nuclear spins are zero) is invariant against the replacement of the atoms [7]. These properties are discussed in [1] in detail.

The lower term, $a^3\Sigma_u^+$, is odd (the *u* subscript). For its symmetric wave function, the rotational states should have the odd quantum numbers of the momentum, $K'' = 1, 3, 5, \ldots$ (the Hund's case *b*). Here, two strokes indicate that the rotational levels of *K*" belong to the lower term, $a^3\Sigma_u^+$.

The upper term, $c^3\Sigma_g^+$, is even (the *g* subscript) and thus differs in parity from the lower term, $a^3\Sigma_u^+$. For its symmetric wave function, the rotational states should have the even quantum numbers of the momentum, $K' = 0, 2, 4, \ldots$. One stroke indicates that the rotational levels of *K*' belong to the upper term, $c^3\Sigma_g^+$.

ELECTRON-VIBRATIONAL-ROTATIONAL TRANSITIONS OF $c^3\Sigma_g^+ \Rightarrow a^3\Sigma_u^+$ SYSTEM

At the molecule transition from one state, *K*', to another, *K*", change in the quantum number, *K*, is defined as $\Delta K = K' - K''$ [8]. The selection rules of the angular momentum change, ΔK, for the radiative transitions divide those transitions into three branches:

—for the transitions of the *P*-branch of the spectrum, $\Delta K = -1$ and the lower level momentum, *K*", is related to the upper level momentum, *K*', as $K'' = K' + 1$;

—for the *R*-branch of the spectrum, $\Delta K = +1$ and $K'' = K' - 1$;

—for the *Q*-branch of the spectrum, $\Delta K = 0$ and $K'' = K'$.

Yet, in the spectra of the $c \Rightarrow a$ and the $C \Rightarrow A$ transitions, the *Q*-branch lines are absent, because in the upper (the odd *K*' numbers) and the lower (the even *K*" numbers) terms, the rotational levels with the identical *K*-numbers are absent.

Figure 3 shows the layout of the rotational levels of the $c^3\Sigma_g^+$ and the $a^3\Sigma_u^+$ triplet terms and of transitions between them. Each *K*-level of the triplet terms is degenerate and contains three levels (the multiplet) with different values of quantum number *J*, the total momentum of the molecule taking into account the spin: $J = K - 1$, $J = K$, $J = K + 1$ [7]. The energy separating these three levels is small. Thus, we will unite the three levels of the multiplet under the united number, *K*. The transitions take place between the levels *J*'

and J'' of the upper and the lower multiplets, K' and K''. The selection rules are defined by the J numbers of the $J' \Rightarrow J''$ transitions.

The transitions are usually designated by the quantum number of the K'' momentum of the lower transition level. To calculate the population of the upper rotational level with the momentum of K', the line intensities and the Hönl–London factors as the functions of the upper level momentum, K', are required. In the majority of the books and the papers available, all these parameters are presented as the function of the K'' number. The interconnection of K' and K'' differs for the different spectrum branches, and the calculations should be performed separately for the different branches.

WAVELENGTHS OF THE ELECTRON-VIBRATIONAL-ROTATIONAL LINES OF THE $c^3\Sigma_g^+ \Rightarrow a^3\Sigma_u^+$ SYSTEM

We took the values of the spectral constants, B_e and α, from [6, 8–10]. The spectral parameters for the studied triplet state at $\nu = 0$ [6, 10] are $B_\nu(c^3\Sigma) = 6.86$ cm^{-1}, $B_\nu(a^3\Sigma) = 7.59$ cm^{-1}, $D_\nu(a^3\Sigma) = 5.62 \times 10^{-4}$ cm^{-1}, and $D_\nu(c^3\Sigma) = 5.58 \times 10^{-4}$ cm^{-1}.

The $K' = 0$ level is the "zero energy" for the upper state, $c^3\Sigma_g^+$, and, the $K'' = 1$ level, for the lower state, $a^3\Sigma_u^+$. The energy between those levels is 10 889.48 cm^{-1} [9], corresponding to the wavelength of 918.32 nm; It is the "center" of the band corresponding to the sequence 0 of the $c^3\Sigma_g^+ \Rightarrow a^3\Sigma_u^+$ system.

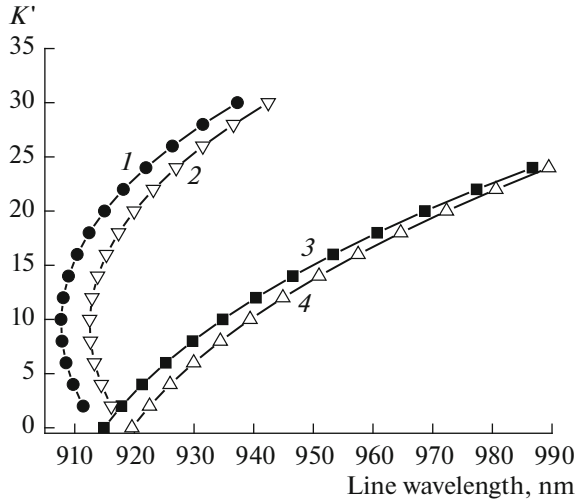

Fig. 4. Wavelengths of the spectral lines with the K' numbers: *1*—the R singlet; *2*—the R triplet; *3*—the P singlet; *4*—the P triplet.

The formulas for the EVR-line wavelengths as the functions of the number, K', of the upper transition level are presented in [1] for the singlet, $C \Rightarrow A$, and the triplet, $c \Rightarrow a$, transitions. Here, we present the formulas for the wavelengths of the P- and R-branch lines (in nm) for $c^3\Sigma_g^+ \Rightarrow a^3\Sigma_u^+$ system:

$$\lambda_P(K') = \frac{918.32}{\left(1 + \dfrac{6.86K'(K'+1) - 7.59(K'+1)(K'+2) + 22.4\times10^{-4}(K'+1)^3}{10889.48}\right)},$$

$$\lambda_R(K') = \frac{918.32}{\left(1 + \dfrac{6.86K'(K'+1) - 7.59(K'-1)K' - 22.4\times10^{-4}(K'+1)^3}{10889.48}\right)}.$$

Figure 4 shows the calculation result for the EVR-line wavelengths with the different K' numbers; here, we present the wavelengths and the line numbers, K', of the singlet, $C \Rightarrow A$, and the triplet, $c \Rightarrow a$, transitions and of the different branches within a wide range of K' values.

Each point in Fig. 4 corresponds to a spectral line; its coordinates indicate the wavelength (the abscissa) and the number, K' (the ordinate). For example, the wavelength range of 930–940 nm includes the P-branch lines of the singlet, $C \Rightarrow A$, and the triplet, $c \Rightarrow a$, transitions with K' numbers from 5 to 12 and the R-branch lines with numbers from 25 to 30. Many R-lines, both of the singlet, $C \Rightarrow A$, and the triplet, $c \Rightarrow a$, transitions are concentrated within the wavelength range of 906–920 nm; thus, their identification is hindered. The line broadening increases with the gas density increase and the lines overlap. That very line overlapping is possibly a source of the continuous background in the spectrum within that wavelength range.

The line positions calculated for the P- and the R-branches of the studied singlet and triplet systems coincide with the data in [6, 9]. The rotational levels are not equidistant; thus, the lines with the same K' number, but belonging to different spectrum branches, have a different wavelength. The P-branch lines are shifted to the red side with respect to the group center at 918.32 nm; and the $K'(\lambda)$ function increases monotonously for the P-branch lines. The R-branch line wavelengths first decrease and then increase. Saturation with the EVR-lines is observed within the wave-

length range of 906–920 nm; here, the identification of the lines from the experimental spectrum is difficult.

The lines having the same K' number but belonging to the different electron radiative states (singlet or triplet) somewhat differ in the wavelength (Fig. 4). This fact is a result of the small difference in the values of the spectral constants of those states. The lines from the different states do not overlap because, in our experiments, the intensities of the singlet system EVR-lines are low. Here, the spectrum shown in Fig. 1 consists of the triplet system lines whereas the singlet system lines do not stand out against the noise background within the studied wavelength range in the corona discharge.

Intensity of the EVR line with the K' number is the product of the upper level population by the Hönl–London factor, $S(K')$, of the transition of this line. For the $c^3\Sigma_g^+ \Rightarrow a^3\Sigma_u^+$ system, the intensity of the line with the upper level number of K' is the sum of the intensities of the three multiplet lines with different J numbers. In [11], the Hönl–London factors are given for the $J' \Rightarrow J''$ transitions as the function of the J'' number. When the relation of the K' and J'' numbers for the P-branch multiplet transitions is known, we obtain the Hönl–London factors as the functions of the upper level number, K':

$$S_P(K') = \frac{(K'+1)(2K'+5)}{(2K'+3)} + \frac{(K'+2)K'}{(K'+1)} + \frac{(K'+1)(2K'-1)}{(2K'+1)} \approx 3.12K' + 1.67.$$

We use this approximation in further calculations. A similar argument for the Hönl–London factors for the R-transitions between the triplet states yields

$$S_R(K') = \frac{(2K'+3)K'}{(2K'+1)} + \frac{(K'+1)(K'-1)}{K'} + \frac{(2K'-3)K'}{(2K'-1)} \approx 3.13K' - 1.25.$$

Figure 5 shows the Hönl–London factors for the P- and the R-branches of the triplet $c \Rightarrow a$ transition and their approximations depending on the K' number of the upper level of the transition.

The number of excited molecules, $n^*(K')$, in the EVR-state with the K' momentum divided by the total number of the excited molecules is the population of the K' rotational level of the $c^3\Sigma_g^+$ state. We might calculate it from the intensity of the K' rotational line measured within the triplet system band. The relative intensity, $I(K')$, of the rotational K' line and the population, $n^*(K')$, of the K' rotational level of the upper state, $c^3\Sigma_g^+$, are related by the expressions

$$I_P(K') \propto (3.115K' + 1.667)n^*(K'), \quad K' = 0,2,4,\ldots;$$
$$I_R(K') \propto (3.125K' - 1.25)n^*(K'), \quad K' = 2,4,\ldots$$

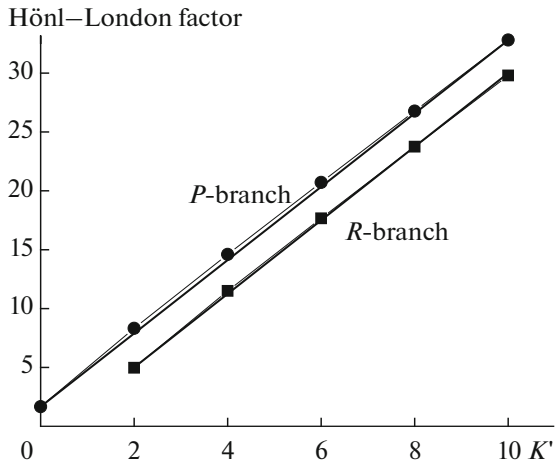

Fig. 5. The Hönl–London factors of the P- and the R-branch transitions of the $c^3\Sigma_g^+ \Rightarrow a^3\Sigma_u^+$ triplet: comparison of the exact values (the dots) and the approximations (the lines).

for the lines of the P- and the R-branches of the triplet $c \Rightarrow a$ transition, respectively.

The Hönl–London factors are the increasing functions of the rotational number K'. The populations of the levels under thermodynamic equilibrium conditions decreases exponentially with the K' increase. Thus, the intensity of the spectral lines in the equilibrium conditions is maximal for transitions with small K'.

In the nonequilibrium plasma of the corona discharge, the situation is different. Analysis of the measured band line intensities of the sequence 0 of the $c^3\Sigma_g^+ \Rightarrow a^3\Sigma_u^+$ system in the supercritical helium gas at 6 K is based on the data presented in Figs. 1 and 6. The cryogenic gas density is low and the line broadening is less than the measurement error. The wavelengths (the spectral position) of the P-branch lines of the triplet $c \Rightarrow a$ transition and their numeration are shown in Fig. 1. The identification (the K' number) of the lines is performed by means of comparison of their wavelengths in vacuum [5]. The high intensive lines are located both in the wavelength range of 950–980 nm (the P-branch lines) and within the range of 910–920 nm (the R-branch lines) and have the same numbers from 14 to 22.

Figure 6 shows the wavelength range of 910–930 nm with the rather intensive lines. The R-branch band lines, sequence 0, of the triplet system with the K' numbers within the range of 10–22 are located there. The R-branch band lines, sequence 0, of the singlet are also located there but their intensity is low.

The K' line numbers are needed to determine the Hönl–London factors of the transition. Here, all the populations are calculated according to the known formulas and are presented in Fig. 7 in the logarithmic scale, depending on the $K'(K' + 1)$ product. In those

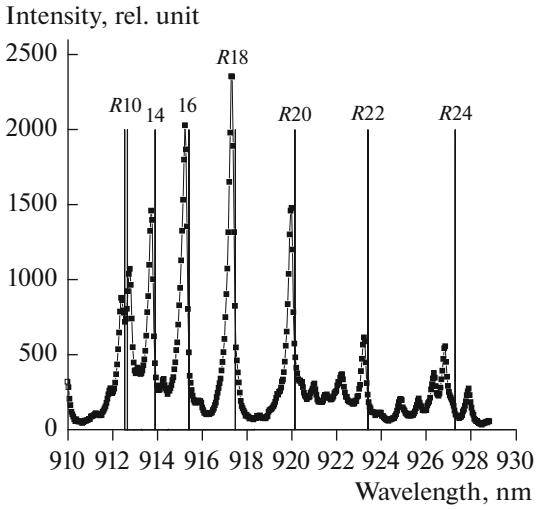

Fig. 6. Location of the *R*-branch lines of $c^3\Sigma_g^+ - a^3\Sigma_u^+$ triplet near 917 nm: the dots—experimental spectrum at 6 K and 0.1 MPa; the vertical bars—the line position in vacuum.

coordinates, the Boltzmann distribution is the straight line. The experimental distribution does not correspond to the Boltzmann distribution and is described by the nonmonotonous function with the maximum at $K' = 18$.

POPULATIONS OF THE ROTATIONAL LEVELS OF THE METASTABLE LOWER STATE, $a^3\Sigma_u^+$

The authors of [12] present other experimental data on the spectrum within the wavelength range of 910–970 nm. A beam of superfluid helium droplets was pierced by a fast electron beam. The excited molecules resided on the droplet surface and moved with them. After the pass, only molecules with a long lifetime, such as the excimers in the $a^3\Sigma_u^+$ metastable state, remained. Then, the droplets were irradiated by a preset frequency laser beam (the photon beam). Under the photon impact, the molecules transited into the excited state, $c^3\Sigma_g^+$, became unstuck from the droplets with the emission of electrons, and the number of those electrons was measured. The electrons gathered on the anode and formed the signal in which the amplitude is plotted over the ordinate axis in Fig. 8. If the laser frequency coincides with that of the transition between the electron-vibrational-rotational levels of the $a^3\Sigma_u^+$ and the $c^3\Sigma_g^+$ states, then the measured current has a peak with the amplitude proportional to the initial number of the molecules at the rotational level of the $a^3\Sigma_u^+$ metastable state.

The position of the peaks corresponds to the frequencies of the transitions between the EVR-levels of the $a^3\Sigma_u^+$ and the $c^3\Sigma_g^+$ states of the He_2^* molecule. In Fig. 8, these peaks are marked by the numbers of the rotational levels, K'', of the lower state, $a^3\Sigma_u^+$. The *P*-branch peaks are designated by the *P* letters whereas the *R*-branch peaks have no designation. The *P*-branch lines are located within the wavelength interval of 950–965 nm and correspond to numbers $K'' = 15$–19. The *R*-lines with those numbers are localized within the range of 915–920 nm. The amplitude of the measured peaks is proportional to the population of the rotational levels of the $a^3\Sigma_u^+$ metastable state of the helium molecule. From the peak amplitudes, the populations of the rotational levels of the $a^3\Sigma_u^+$ metastable state of the He_2^* excimer are calculated; they are

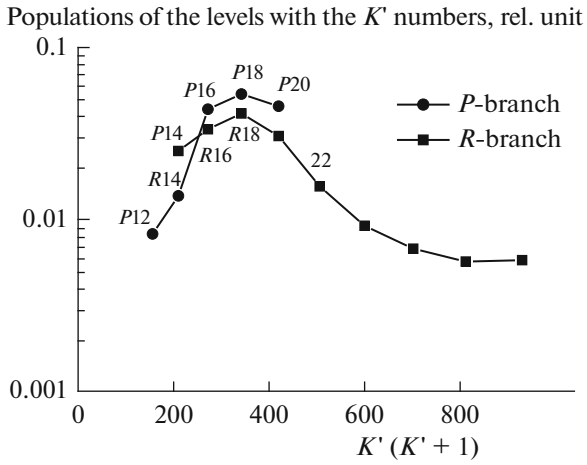

Fig. 7. Populations of the rotational levels of the upper triplet term, $c^3\Sigma_g^+$, obtained from the data on the intensities of the *P*- and the *R*-branch lines of the spectrum emitted by the corona discharge in the supercritical helium gas at 6 K.

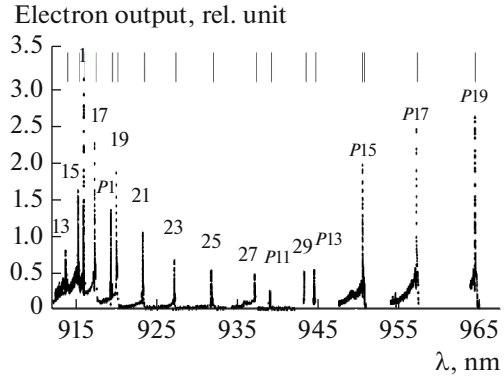

Fig. 8. Output of the secondary electrons as the function of the wavelength of the laser photons exciting the He_2^* molecules from the lower $a^3\Sigma_u^+$ state term to the upper $c^3\Sigma_g^+$ state and detaching the molecules from the liquid droplet surface [12].

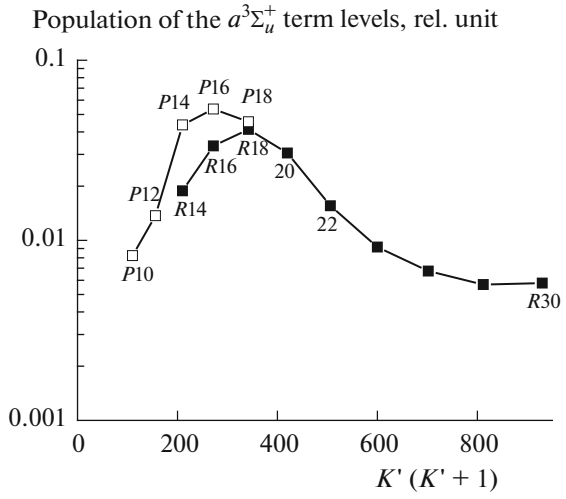

Fig. 9. Population distribution of the rotational levels of the $a^3\Sigma_u^+$ lower metastable term obtained from the analysis of the electron output data (Fig. 8).

shown in Fig. 9 as the function of the number, K', of the upper rotational term of $a^3\Sigma_u^+$. The distribution is nonmonotonous, with the maximum at $K' \approx 18$.

CONCLUSIONS

We created the facility to investigate the corona discharge in helium at cryogenic temperatures within a wide range of thermodynamic states (from the liquid at 4.2 K to supercritical gas at 6–14 K) and various pressures. The intensity of the light emitted by the discharge is sufficient for its spectral analysis. The observed spectra are typical for the spectra emitted by the atom or the molecule surrounded by the domain with low-density medium.

The excited molecules occur within the ionization zone of the corona discharge via the short-range interaction of the excited atoms in the triplet, 2^3S, state with the He atom in the ground state. In the liquid He, both excited atoms and the excited molecules are surrounded by empty bubbles due to the weak mutual repulsion of the He* and the He atoms to a distance above 5 Å [14] with the potential of 100 cm^{-1} in the maximum. The bubble existence is the conventional model to describe the peculiarities of the atomic spectra of the liquid helium [4, 5, 13–17]. Sufficient blue shift of the spectral lines comparable to the line broadening is a typical indication of the fact that the emitting atom is inside the bubble. In the other limiting case of rarefied gases, the line shape and position are governed by the collisional interaction with the surrounding atoms and the line shift is always less than their width.

We observed the spectra of the radiative transitions corresponding to the singlet, $A \Rightarrow C$, and the triplet, $a \Rightarrow c$, systems in the experiments in the liquid helium at the temperature of 4.2 K. These spectra are very poor in lines as compared against the spectra of the supercritical gas at 6 K. In the liquid, the spectra consist of several broadened electron-vibrational-rotational lines belonging to the different states and branches. All the observed lines have the numbers $K' = 0, 2, 4$. This fact means that only those levels have noticeable populations decreasing with the K' number increase.

In the spectrum of the corona discharge in the gas at 6 K, we observed in fact all the lines with the numbers $K' < 26$. These lines are within the wavelength range of 910–990 nm. The lines belong to the different branches, predominantly to the transition between the triplet states. We observed two groups of the high intensive lines belonging to the P- and the R-branches. Note that these lines (belonging to the different branches and having the different wavelengths) have similar numbers close to $K' \approx 18$. This fact is a consequence of strong nonequilibrium in population of the rotation levels. The population distribution is described by the nonmonotonous function of the rotational quantum number, K'.

The analysis of the rotational spectrum of the transitions between the $a^3\Sigma_u^+$ and the $c^3\Sigma_g^+$ states proposed in the present paper was applied to the results of the experiment [12] where the authors registered the spectrum of photo-detachment of the excimer molecules from the superliquid helium microdroplets. The results of our experiments and [12] add to each other. In our experiments, we obtained the nonmonotonous distribution of population of the rotational levels of the $c^3\Sigma_g^+$ term in the corona discharge in cryogenic gas at 6 K. The authors of [12] obtained the same distribution for the $a^3\Sigma_u^+$ term levels under the irradiation of the superliquid HeII micro-droplets by the electron beam at 1.7 K.

ACKNOWLEDGMENTS

The authors V.M. Atrazhev and V.A. Shakhatov are grateful to the Russian Foundation for Basic Research for the support, project no. 12-016-91052.

REFERENCES

1. Atrazhev, V.M., Shakhatov, V.A., Boltnev, R.E., Bonifaci, N., Aitken, F., and Eloranta, J., *High Temp.*, 2017, vol. 55, no. 2, p. 165.
2. Li, Z., Bonifaci, N., Denat, A., Aitken, F., von Haeften, K., Atrazhev, V.M., and Shakhatov, V.A., *IEEE Trans. Dielectr. Electr. Insul.*, 2009, vol. 16, p. 742.
3. Dennis, W.S., Durbin, E., Fitzsimmons, W.A., Heybey, O., and Walters, G.K., *Phys. Rev. Lett.*, 1969, vol. 23, no. 19, p. 1083.
4. Soley, F.J. and Fitzsimmons, W.A., *Phys. Rev. Lett.*, 1974, vol. 32, p. 988.
5. Von Haeften, K., Laarmann, T., Wabnitz, H., and Moller, T., *Phys. Rev. Lett.*, 2002, vol. 88, p. 233401.

6. Focsa, C., Bernath, P.F., and Colin, R.J., *J. Mol. Spectrosc.*, 1998, vol. 191, p. 209.
7. Landau, L.D. and Lifshits, E.M., *Kvantovaya teoriya. Nerelyativistskaya teoriya* (Quantum Theory. Nonrelativistic Theory), Moscow: Nauka, 1974.
8. Kovacs, I., *Rotational Structure in the Spectra of Diatomic Molecules*, London: Adam Hilger, 1962.
9. Herzberg, G., *Molecular Spectra and Molecular Structure*, vol. 1: *Spectra of Diatomic Molecules*, Princeton: Van Nostrand Reinhold, 1950.
10. Smirnov, B.M., *Atomnye stolknoveniya i elementarnye protsessy v plazme* (Atomic Collisions and Elementary Processes in Plasma), Moscow: Atomizdat, 1968.
11. Schadee, A., *Bull. Astron. Inst. Neth.*, 1964, vol. 17, p. 311
12. Yurgenson, S., Hu, C.-C., Kim, C., and Northby, J.A., *Eur. Phys. J. D*, 1999, vol. 9, p. 153.
13. Hickman, A.P., Streets, W., and Lane, N.F., *Phys. Rev. B: Solid State*, 1975, vol. 12, p. 3705.
14. Bonifaci, N., Aitken, F., Atrazhev, V.M., Fiedler, S.L., and Eloranta, J., *Phys. Rev. A: At., Mol., Opt. Phys.*, 2012, vol. 85, 042706.
15. Shakhatov, V.A. and Lebedev, Yu.A., *High Temp.*, 2015, vol. 50, no. 5, p. 658.
16. D'yachkov, L.G., *High Temp.*, 2016, vol. 54, no. 1, p. 5.
17. Babaeva, N.Yu., Berry, R.S., Naidis, G.V., Smirnov, B.M., Son, E.E., and Tereshonok, D.V., *High Temp.*, 2016, vol. 54, no. 5, p. 745.

Translated by I. Dikhter